Available online at www.sciencedirect.com
ScienceDirect
Cement and Concrete Research 36 (2006) 2098–2102
Cement and Concrete Research

Macrocell and microcell corrosion of steel in ordinary Portland cement and high performance concretes

C.M. Hansson *, A. Poursaee, A. Laurent

Department of Mechanical Engineering, University of Waterloo, Waterloo, Ontario, Canada N2L 3G1

Received 23 October 2005; accepted 17 July 2006

Abstract

Microcell corrosion is the term given to the situation where active corrosion and the corresponding cathodic half-cell reaction take place at adjacent parts of the same metal. Macrocell corrosion can occur when the actively corroding bar is coupled to another bar which is passive, either because of its different composition or because of different environment. The present study was undertaken to determine the influence of concrete type and properties on the relative microcell and macrocell corrosion rates. The samples were monitored for more than 3 years and the results confirm that microcell corrosion is the major mechanism in corrosion of steel reinforcing bars in concrete. Furthermore, results show that, for high performance concrete, the difference between microcell and macrocell corrosion is far more significant than for ordinary Portland cement concrete because of its high resistance to ionic flow.

Keywords: Microcell corrosion; Macrocell corrosion; Durability; Electrochemical properties; High-performance concrete

1. Introduction

The various definitions of macrocell and microcell have been discussed by Rodriguez et al. [1]. For the purpose of this paper and following the convention used in practice, microcell corrosion is the term given to the situation where active dissolution and the corresponding cathodic half-cell reaction (the reduction of dissolved oxygen) take place at adjacent parts of the same metal part, as illustrated in Fig. 1. For steel reinforcing bar (rebar) in chloride-contaminated concrete, this process always occurs in practice, for example, in specimens in the laboratory containing a single bar and in structures reinforced with a single rebar mat. As will be shown in this paper, it is the dominant corrosion process in case where there are multiple rebars layers.

Macrocell or galvanic corrosion can occur when the actively corroding bar is coupled to another bar which is passive or has a lower corrosion rate, either because of its different composition or different environment. An example of the former situation is black steel in chloride-contaminated concrete and in contact with stainless steel; the latter situation can occur when a top black steel mat in chloride-contaminated concrete is coupled to a bottom black steel mat in chloride-free concrete, as illustrated in Fig. 2. Macrocells can also form on a single bar exposed to different environments within the concrete or where part of the bar extends outside the concrete. The process is the same in all cases and, in all cases, the corrosive action of the macrocell is added to that of the microcells.

It should be emphasised that the simplified view of the "active steel becoming the anode and the passive steel becoming the cathode" is not actually correct. In each of these cases, the anodic and cathodic reactions occur on both metal surfaces; when the two metals are coupled, the anodic corrosion of the more active

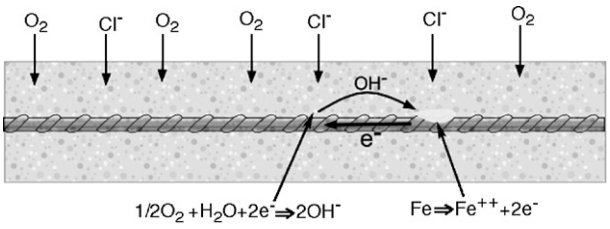

Fig. 1. Schematic illustration of microcell corrosion.

* Corresponding author. Tel.: +1 519 8884538.
E-mail address: chansson@uwaterloo.ca (C.M. Hansson).

0008-8846/$ - see front matter © 2006 Elsevier Ltd. All rights reserved.
doi:10.1016/j.cemconres.2006.07.005

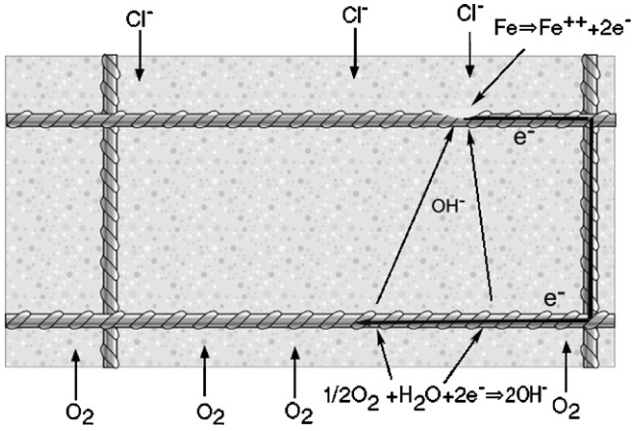

Fig. 2. Schematic illustration of macrocell corrosion.

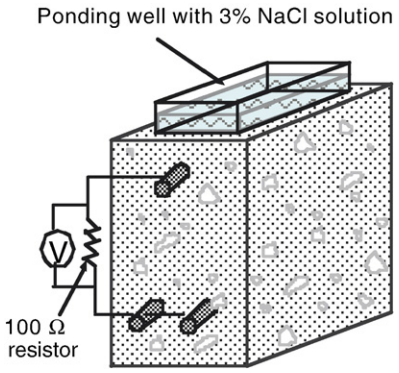

Fig. 3. ASTM G-109 specimen.

metal increases while that of the less active or passive metal decreases, and vice versa for the cathodic reactions.

While a macrocell corrosion current can be measured directly, the same is not true of microcell corrosion and, therefore, many investigators choose to neglect the microcell component. This has led to the general assumption that macrocell corrosion is always the dominant component. However, Andrade et al. [2] have analysed the relative contributions of microcells and macrocells. They concluded that the influence of the macrocell only becomes significant, i.e. of the same order as the microcell corrosion, when the ratio of surface areas of the passive/active regions is greater than approximately 50 : 1. Moreover, these authors concluded that the theoretical maximum effect (with an infinitely large cathode and infinitely small anode) would be an increase in active corrosion rate of only 2–5 times that of the microcells alone. Similarly, Trejo and Monteiro concluded that the difference between the corrosion mass loss measured gravimetrically and that calculated from macrocell corrosion rate measurements must be due to the microcell corrosion [3]. In another study of macrocell corrosion, Suzuki et al. [4] concluded that the maximum anodic dissolution rate of the steel in concrete was the limiting rate controlling factor not the anode/cathode area ratio. Furthermore, corrosion of the rebar is typically a localised attack, occurring over only part of the length of the bar and often over only part of the circumference. The contribution of the passive area of the bar towards the cathodic half-cell reaction is not taken into account if only macrocell currents are measured.

The present study was undertaken to determine the influence of a number of parameters, particularly, concrete properties and reinforcing bar type, on the relative micro- and macrocell corrosion rates. This paper documents the influence of concrete properties.

2. Experimental procedure

A standard ASTM specimen design [5] was used for determination of the relative corrosion protection provided by the different concretes using macrocell corrosion measurements. The specimen is illustrated schematically in Fig. 3 and consists of a concrete prism, 279 mm × 152 mm × 114 mm (11 in. × 6 in. × 4.5 in.) containing three lengths of 10M reinforcing bar (rebar): one bar at the top with a cover depth of 25 mm and two at the bottom, also with a cover depth of 25 mm. The rebars were degreased but the mill scale was left intact. To prevent extraneous effects, the ends of the bars were coated with epoxy resin to define the exposed length (203 mm of the 279 mm of the bar within the concrete). Seven prisms were cast from each of three concrete mixtures: an ordinary Portland cement concrete (OPCC) corresponding to CSA Class C-2, and two high performance concrete (HPC) mixtures designed to meet the specifications of the Ministry of Transportation of Ontario (MTO) which require the sue of silica fume cement and permit the use of up to 25% cement replacement by either blast furnace slag or class C fly ash [6]. The concretes were provided by Dufferin Concrete and their mixture proportions are given in Table 1.

In addition to the prisms, cylinders (100 mm Φ × 200 mm) were cast for compression tests and rapid chloride permeability. After placement, all specimens were cured under wet burlap and plastic according to the MTO specifications, i.e. 2 days for the OPCC and 7 days for the HPCs. The specimens were then stored outdoors for 5 months (June to October 2001) prior to preparation for exposure to chlorides.

Table 1
Mixture constituents per cubic metre of concrete

	OPC	HPC/S	HPC/F
Type 10 Portland (kg)	355	–	–
Type 10SF Portland (kg)	–	337	337
Slag (kg)	–	113	–
Fly ash (kg)	–	–	113
Sand (kg)	770	718	718
Stone 20 mm (kg)	1070	1065	1065
Water (l)	153	158	158
Eucon MRC air entrainment	40 ml/100 kg cementitious	65 ml/100 kg cementitious	65 ml/100 kg cementitious
Water reducer	250 ml/100 kg cementitious	250 ml/100 kg cementitious	250 ml/100 kg cementitious
Superplasticizer	–	2 l + 1.5 l	3 l + 0.5 l
W/CM ratio	0.43	0.35	0.35

The prism specimens were prepared for corrosion measurements as follows:

i. the vertical surfaces were coated with epoxy resin to prevent access of oxygen from those surfaces;
ii. a ponding well was mounted on the top surface; and
iii. the two bottom bars were connected together and then connected to the top bar through a 100 Ω resistor.

The ponding well was filled with a 3 wt.% NaCl solution and the specimens were alternately exposed to 2-week periods with solution then 2 weeks without solution. The voltage drop across the resistor was monitored daily allowing the macrocell corrosion current between the top (anode) bar and the bottom (cathode) bar to be determined using Ohm's law.

After 180 weeks of macrocell measurements, the microcell corrosion rate of the top bar was determined by the linear polarization resistance (LPR) technique [7] using a saturated calomel reference electrode and a stainless steel counter electrode immersed in the ponding solution. Thereafter, the top bar was disconnected from the bottom bars and, after being allowed to stabilize for a week, the microcell corrosion rate was measured again.

3. Results and discussion

The 28-day compressive strengths and rapid chloride permeabilities (RCP) of the three concretes are given in Table 2. The data show that the two high performance concretes do fulfil the MTO specifications of >50 MPa and the HPC/S fulfils the ASTM C1202 specification. The HPC/F is 6% lower that the ASTM C1202 limit at 28 days due to the slow pozzolanic reaction of the fly ash but fulfils the specification at 56 days. The electrical resistivities of the concretes determined from the initial RCP data are included in Table 2 and show significantly higher values for the two HPCs than for OPCC.

The macrocell data are given in Fig. 4 and it should be noted that the ordinate scale for the steel in OPCC is an order of magnitude greater than that for the steel in the two HPCs.

Thus, the data show a very significant improvement in the protection afforded to steel by the use of HPC than the OPCC: for both types of HPC, there is no indication of active corrosion after 180 weeks exposure to chlorides. However, the corrosion initiation times for the OPCC range from 35 days to 140 weeks. This wide range is illustrative of the variations in chloride ingress and corrosion initiation observed in practice, which are a function of the inhomogeneity of the concrete microstructure and of the passive film on the steel. A specific corrosion current density corresponding to active corrosion initiation cannot be defined because of these inhomogeneities and the consequent lack of any way of determining the area of active corrosion.

Table 2
Physical properties of concretes

Property	Age (days)	OPC	HPC/S	HPC/F
Compressive strength (MPa)	28	41.1	59.5	59.3
	56	42.2	51.6	55.4
ASTM C1202 Coulombs passed in 6 h	28	6128	942	1060
	56	5938	701	799
Electrical resistivity (kΩ cm)	28	3.5	20.9	19.4
	56	4.0	28.6	24.7

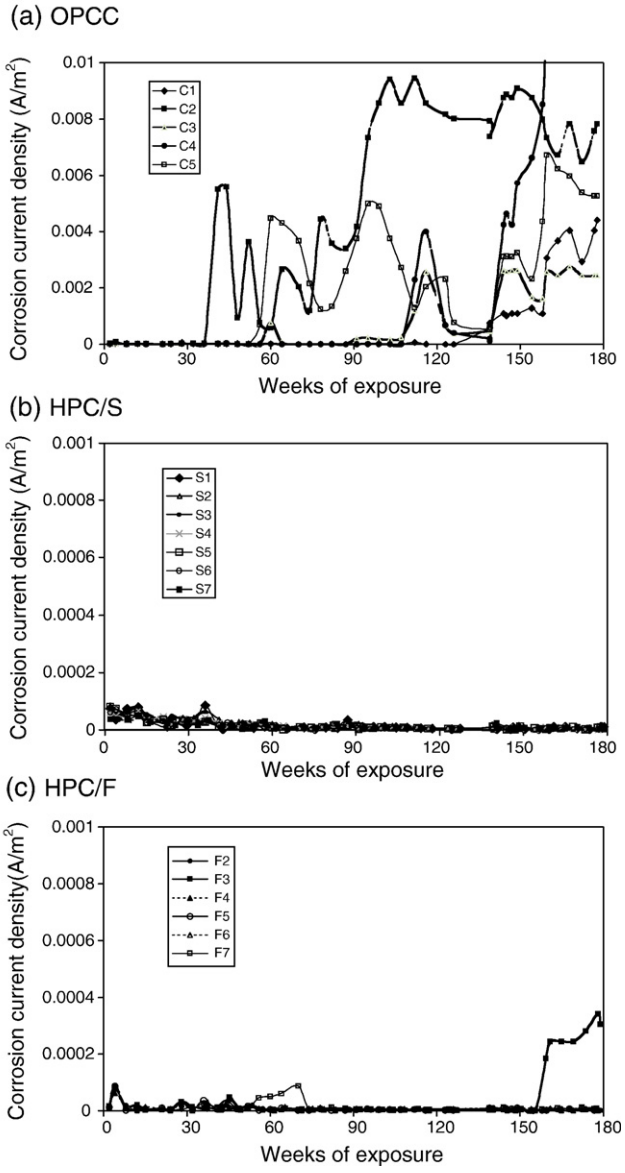

Fig. 4. Macrocell corrosion current density as a function of exposure to chlorides. Note that the ordinate scale for the OPC (a) concrete specimens is 10 times greater than that for the two HPCs (b, c).

The macrocell current densities after 180 weeks exposure are plotted against the microcell current densities measured at the same time for the individual prisms with the top bar connected to the bottom bars in Fig. 5 and for the top bars disconnected in Fig. 6. It should be noted that there is more scatter in the data in Fig. 6 than those in Fig. 5 and this is attributed to the fact that some of the specimens may not have fully stabilized after disconnection.

For the OPCC prisms, the microcell corrosion rates are only ~2 times greater than that of the macrocell corrosion rates

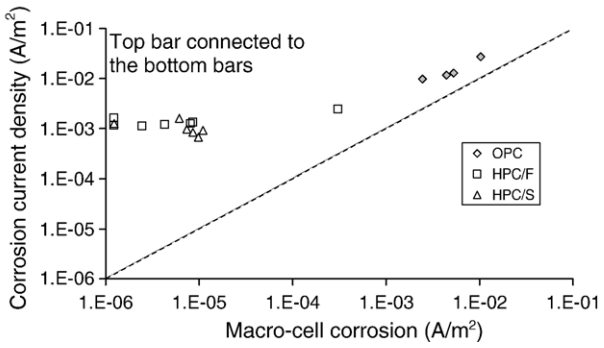

Fig. 5. Comparison between the macrocell and microcell corrosion current densities for the steel in OPCC and HPC specimens.

indicating that the overall corrosion – the sum of macrocell and microcell currents – is about 3 times that measured by macrocell measurements alone. On the other hand, while the macrocell corrosion rates of steel in HPC ($<10^{-5}$ A/m^2) are three to four orders of magnitude lower than that in OPCC ($\sim 10^{-2}$ A/m^2), their microcell current densities ($\sim 10^{-3}$ A/m^2) are only about one order of magnitude lower than that in OPCC ($<10^{-2}$ A/m^2). In other words, the macrocell current in HPC is between two and three orders of magnitude lower than the microcell values and can effectively be ignored in considering the overall corrosion of steel in HPC. This is not surprising because macrocell currents are controlled, in large part, by the resistance to an ionic current flow in the concrete between the top bar and the bottom bars which, as indicated by data in Table 2, is much higher in the HPCs than in the OPCC. For microcell corrosion, on the other hand, the anodic and cathodic half-cell reactions can take place at adjacent locations (on a microscopic scale) on the bar and require very short ionic current paths.

Samples of the top bar from each of the three concretes, shown in Fig. 7, illustrate the significantly greater susceptibility of steel to corrosion when embedded in OPCC concrete than when embedded in either HPC. The small amount of corrosion in the steel from this particular HPC/F specimen (HPC/F-3) is detectable in the rise in corrosion rates observed in Fig. 4(c). It is interesting to note that the original mill scale is no longer evident on the bars after 4 years embedded in

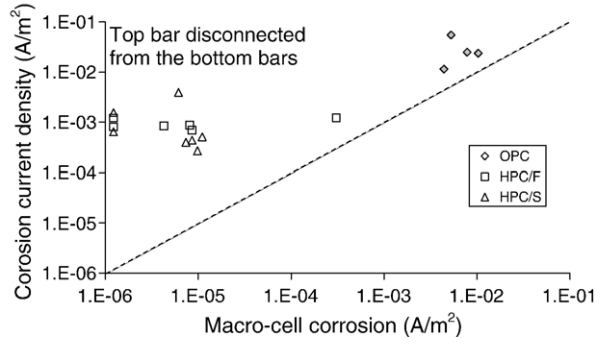

Fig. 6. Comparison between the macrocell and microcell corrosion current densities for the steel in OPCC and HPC specimens when the top bars are disconnected from the bottom bars.

Fig. 7. Top steel rebar recovered from three of the G-109 concrete specimens after 185 weeks of exposure to chlorides.

concrete. An explanation of this phenomenon is currently under investigation.

The OPCC data are in qualitative agreement with previous studies [2] except for the area ratio of "cathode" and "anode". As shown in Fig. 7, the area of intense active corrosion is approximately 20% of the top bar and there are also many small pits along the rest of the bar. This would give a ratio of non-corroding (cathodic) area (i.e. the non-corroding area of the top bar plus the total area of the two bottom bars) to corroding (anodic) area of only about 10:1 while the macro- and microcell corrosion rates are the same order of magnitude. On the other hand, the HPC data show vastly different orders of magnitude for micro- and macrocell corrosion, and would require a huge cathode/anode area ratio for similar levels of the two types of corrosion. This illustrates yet another advantage of the HPC over OPCC, namely the ability to make the effects of connection between rebar mats to be insignificant. Moreover, the data indicate the danger of relying on macrocell measurements to determine the onset and extent of corrosion, as also noted by Rodriguez et al. [1].

4. Summary and conclusions

1. For black steel in CSA Class C-2 OPCC with a relatively low electrical (ionic) resistance, the macrocell and microcell corrosion components are of the same order of magnitude and can be added together to provide the total corrosion rate on the actively corroding bar. In this case, the total corrosion rate was approximately three times that of the macrocell rate alone.
2. In contrast, the macrocell corrosion of black steel in HPC is negligible and the corrosion is limited to microcells on the top bar by the ionic resistance of the concrete.
3. The microcell corrosion rate is approximately one order of magnitude lower in HPC that in OPCC. This may be attributed due to the fact that the chloride level at the top reinforcing bar is lower in HPCs than in OPCC because of the difference in chloride diffusion rates.
4. Care must be taken in using the results of macrocell measurements. The absence of macrocell corrosion cannot be taken as an indicator that microcell corrosion is not occurring. This is particularly true for HPC where measured macrocell corrosion rates may be very small.
5. The behaviour of HPC containing 25% fly ash and HPC containing 25% slag, is very similar so there is no apparent advantage to the use of one or the other.

6. The advantages of lower macrocell effects and, consequently, the limitation of galvanic effects for metals in HPC can be added to the other attributes of the high performance concretes, namely higher strength and greater resistance to chloride ingress through diffusion.

Acknowledgements

Support for this project was provided by the Cement Association of Canada, the Natural Sciences and Engineering Research Council of Canada and Materials and Manufacturing Ontario. The authors are grateful to St. Lawrence Cement, Lafarge Canada and Dufferin Concrete for providing the materials, to Mr. Richard Morrison and Mr. Doug Hirst for technical assistance and to Dr. Laura Mammoliti for extensive discussions of the results.

References

[1] P. Rodriguez, E. Ramirez, S. Feliu, J.A. Gonzalez, W. López, Significance of coplanar macrocells to corrosion of concrete-embedded steel, Corrosion 55 (3) (1999) 319–325.

[2] C.M. Andrade, I.R. Feliu, S. Gonzalez, J.A. Feliu, J.S. Feliu, The effect of macrocells between active and passive areas of steel reinforcements, Corrosion Science 33 (2) (1992) 237–249.

[3] D. Trejo, P.J. Monteiro, Corrosion performance of conventional (ASTM A615) and low-allow (ASTM A706) reinforcing bars embedded in concrete and exposed to chloride environments, Cement and Concrete Research 35 (2005) 562–571.

[4] K. Suzuki, Y. Ohno, S. Praparntanatorn, H. Tamura, Some phenomena of macrocell corrosion, Corrosion of Reinforcement in Concrete, Elsevier Applied Science, Wishaw, UK, 1990.

[5] ASTM G109-02, Standard Test Method for Determining the Effect of Chemical Admixtures on the Corrosion of Embedded Steel Reinforcement in Concrete Exposed to Chloride Environments, American Society for Testing Materials, West Conshocken, PA, 1992, pp. 451–455.

[6] OPSS, SSP 904 S13 High Performance Concrete. 1995, Ontario Provincial Standard Specification.

[7] M. Stern, A.L. Geary, Electrochemical polarisation: I. A theoretical analysis of the shape of polarisation curves, Journal of the Electrochemical Society 104 (1) (1957) 56–63.